**VIII International Conference on
Computational Methods for
Coupled Problems in Science and Engineering**

COUPLED PROBLEMS 2019

3-5 June 2019 in Sitges, Spain

Eugenio Oñate, Manolis Papadrakakis and Bernhard A. Schrefler (Eds.)

A PSEUDOTHERMAL APPROACH FOR SIMULATING THE RESIDUAL STRESS FIELD CAUSED BY SHOT BLASTING

STEFANOS GKATZOGIANNIS[*], PETER KNOEDEL AND THOMAS UMMENHOFER

KIT Steel & Lightweight Structures
Research Center for Steel, Timber & Masonry
Otto-Ammann-Platz 1
D-76131 Karlsruhe

Key words: Shot blasting, residual stresses, weld simulation, pseudothermal loading

Abstract. Industrial practice often prescribes cleaning of steel surfaces prior to welding with shot blasting. Shot blasted components have been considered free of residual stresses. Hence, recent studies show that these residual stresses from mechanical surface treatments are not negligible. A simulation of the surface treatments and their mechanical effect in full scale though, is not possible under modern computational capabilities. Instead, a straightforward, pseudothermal approach is proposed and tested in the present study, in order to introduce an initial residual stress field from shot blasting by application of thermal strains. This engineering concept is applied for validation reasons on a small-scale specimen, where a measured profile of residual stresses from shot blasting is simulated with preciseness. Subsequently a component with dimensions of real weldments is modelled, so that simplifications reducing the computational time to acceptable levels can be derived.

LIST OF NOTATIONS

E	Young's modulus (MPa)
f	yielding function
$f_s(u)$	resisting force as a function of displacement u (N)
H	tangent modulus of bilinear σ-ε material behaviour [MPa]
p(t)	external transient loading (N)
T	temperature (°C)
t	time (s)
u	displacement (mm)
ε	strain (-)
α_{se}	secant coefficient of thermal expansion
δ_{ij}	Kronecker's delta
ν	Poisson's ratio (-)
σ	stress (MPa)
$\sigma_{\varepsilon q}$	von Mises effective stress (N/mm^2)

1   INTRODUCTION

Steel plates are usually considered free of residual stresses (RS) prior to welding, although it is well understood that there are RS from the rolling process, especially in the case of cold rolled plates. Nevertheless, significant deviation of simulated welding residual stresses (WRS) with the respective measured profiles was met in an ongoing research project [1]. The investigated component was a fillet weld made of S355 with real yield strength of 400 MPa. It was simulated with a previously validated engineering approach for calculating the WRS of weldments [2], [3], [4] etc. The simulation provided very good agreement with the measurements in the fusion zone (FZ), the heat affected zone (HAZ) and the parent material (PM) near them. However, compressive stresses in an order of magnitude of -200 MPa were met in the PM away from the HAZ, an effect that could not be reflected by the numerical model. The above-mentioned very good agreement of numerical and experimental results near the critical weld section led to the conclusion that the simulation was valid and a different effect than welding should account for these compressive RS.

Previous investigations by Shaw et al. [6] and Hensel et al. [7] have proven that most of the widely applied surface treatments, such as shot blasting or glass peening, lead to the introduction of non-negligible compressive RS on the surface, of a different magnitude in each case though. The through-depth RS profiles, which were measured in [6] for different surface treatments of a mechanical component of a 20MnCr5 steel [8], are presented in Figure 1. This material is reported to exhibit a yield strength of 398 MPa at room temperature, ultimate tensile strength of 562 MPa and Young's modulus of 219 GPa [9]. It becomes evident from these measurements, that even for surface treatments like shot blasting, where no obvious, significant deformation of the surface takes place, non-negligible residual stresses can be introduced. Based on these findings, it was concluded that in the above-mentioned case of fillet welds of S355, shot-blasting, which was applied on the surface of the plates prior to welding to remove the mill scale and foreign matter, had to be accounted for the compressive RS.

In the case presented in [6], the peak RS near the surface were measured to be -329 MPa, i.e. 83 % of the yield limit. In the case of the S355 fillet welds, residual stress profiles with significant deviation in the range of -200 MPa to -300 MPa were measured, fluctuating between 50 % and 75 % of the yield strength. Detailed results will be published in [1], [10]. Such discrepancies are expected, as the profiles were measured on the surface of the specimen and the effect of these surface treatments is localized around the impact locus. Moreover, different batches of 20MnCr5 exhibit significant deviation regarding yield strength, which is predominant for introduced RS, and there is no reference to the strength of the specific applied batch provided in [6].

RS introduced by shot blasting in the weld region are rationally considered to be relieved by the thermal input during subsequent welding. It's becoming evident though that in order to properly simulate WRS away from the weld as well, RS from shot blasting have to be considered in subsequent simulations. Nonetheless, a direct, full-scale simulation of shot blasting treatment is not possible. It would require the simulation of a great number of impacts, raising an unfeasible numerical problem with modern computational capabilities. The present study investigates the possibility of applying a fictitious thermal load in a pseudothermal analysis instead, in order to generate a compressive RS field similar to that of shot blasting. The present method is not foreseen to act predictively but to reproduce measured profiles of residual

stresses from shot blasting as input for the simulation of WRS in existing weldments. Prerequisite is to minimize the computational effort so that it can be applicable in practice.
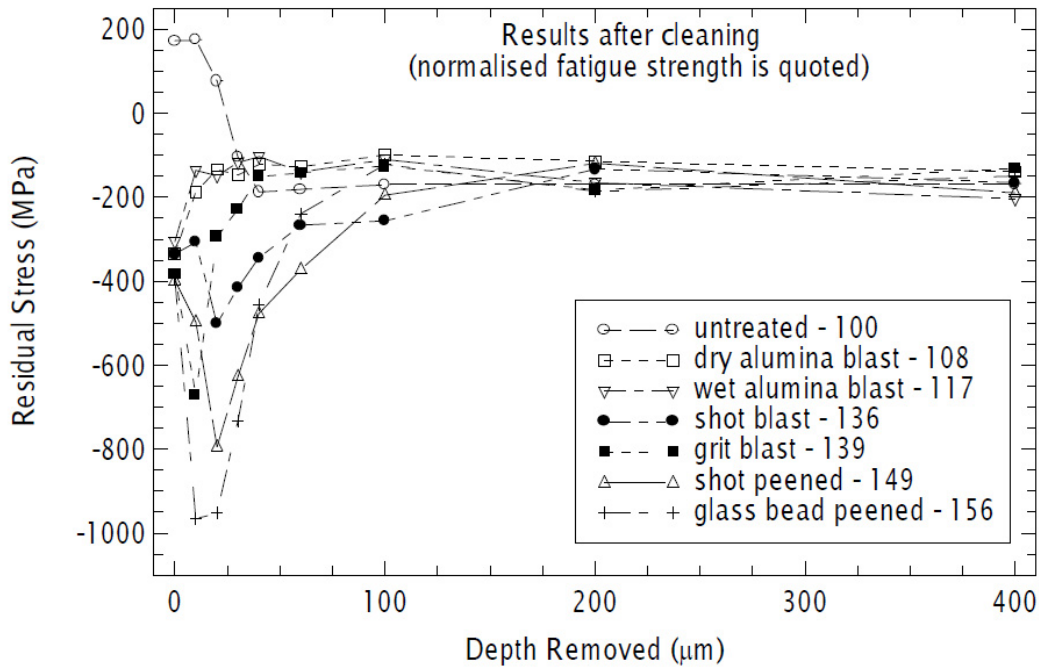

Figure 1: In depth RS profiles introduced by different surface treatments, found in [6]

2 THEORETICAL BACKGROUND

A quasi-static solution is applied for the present study, governed by eq. 1,

$$f_s(u) - p(t) = 0 . \tag{1}$$

Total mechanical strain is decomposed to elastic and plastic parts (eq. 2),

$$\varepsilon_{tot}^{mech} = \varepsilon_{el} + \varepsilon_{pl} . \tag{2}$$

The stress σ is proportional to the elastic strain ε_{el} according to Hooke's law for linear isotropic material behaviour, which is presented in the following equation (eq. 3) in terms of Young's modulus and Poisson's ratio and in tensor notation,

$$\varepsilon_{ij} = \frac{1}{E}(\sigma_{ij} - v(\sigma_{kk}\delta_{ij} - \sigma_{ij})) , \tag{3}$$

where δ_{ij} is the Kronecker delta. Von Mises yield criterion (eq. 4),

$$f(\sigma, \sigma_y) = \sigma_e - \sigma_y = 0, \tag{4}$$

is widely applied for metallic materials, where σ_ε is the von Misses equivalent stress (eq. 5),

$$\sigma_e = \sqrt{\frac{3}{2}\left(\sigma : s - \frac{1}{3}tr(\sigma)^2\right)} . \tag{5}$$

The pseudothermal loading is applied as thermal strains based on the temperature dependent coefficient of thermal expansion α^{se} (5)

$$\varepsilon^{th} = a^{se}(T) \cdot (T - T_{ref}).$$

3 INVESTIGATED CASES

3.1 Proposed approach and previous considerations

Goal of the present study was the generation of RS from shot blasting based on an existing measured profile, which would act as input for subsequent weld simulation. According to textbook knowledge, when an area of a metallic component is heated rapidly like in the case of welding, restraining of the zone from neighbouring cold material leads to the introduction of plastic strains and in extension RS. When no other phenomena such as microstructural transformations that influence their magnitude take place, RS in this area are tensile. This effect can be reproduced by numerical approaches and has been thoroughly investigated by the authors of the present study in the past [2], [3], [4], [5] etc. As the generated profile of RS in the present case should be compressive, it was assumed that the respective area of the component should be cooled contrary to welding. Initial expectations dictated the application of temperature lower than the ambient, which whenever possible would follow the measured RS qualitatively in the depth direction. It was believed that in this way it would be more straightforward to generate the measured RS profile and its peaks and valleys. Once again, according to common knowledge, the magnitude of the introduced RS is higher for a restrained (during the application of heating/cooling) component and therefore, restraints were applied on the faces of the investigated components as described-below. Selection of the restraints was arbitrary and such that would not lead to numerical difficulties, based on previous knowledge of the authors. Finally, it was decided that the RS field after removal of the boundary conditions would be compared with the measured one, as the component with the generated RS profile should be restraint-free for application in subsequent analyses.

3.2 Investigated components

Two components were investigated in the present study; a small-scale one made of 20MnCr5 steel (component A) and a larger one made of S355 (component B). It was evident even before present study that a very fine mesh of the order of magnitude of 10 μm would be needed in order to reproduce RS profiles, which variate significantly at the top 100 μm near the surface. Nevertheless, the same mesh has to be subsequently applied to a weld simulation, whereby modelling of a real size component with this element sizes is not possible under modern computational restrictions. Hence, a component with dimensions of 5 mm x 5 mm x 5 mm and finer mesh was modelled at first. Goal was to validate the feasibility of the method by introducing the through-depth profile of RS from shot blasting measured in [6]. The upper 1 mm of the component was meshed with elements of variating thickness from 0.0025 mm at the top layer to 0.0255 mm at the bottom. Trough-thickness element size was 1 mm for the rest of the component. A universal transverse and longitudinal element dimension of 0.1 mm was applied (x and y direction). Component A along with the respective applied mesh is presented in Figure 2.

Component B had dimensions of 1000 mm x 365 mm x 10 mm, identical with the components investigated in [1]. In this case, as modelling with the above-mentioned mesh is prohibitive for subsequent welding simulations, a simplified approach is proposed alternatively. A universal element size of 0.3 mm is applied, which is of the same order of magnitude with the mesh in the HAZ during weld simulations. It is assumed for the present study that only 100 mm adjacent to the weld line in both directions are shot blasted. Component A along and the respective applied mesh are presented in Figure 3 and 4 respectively.
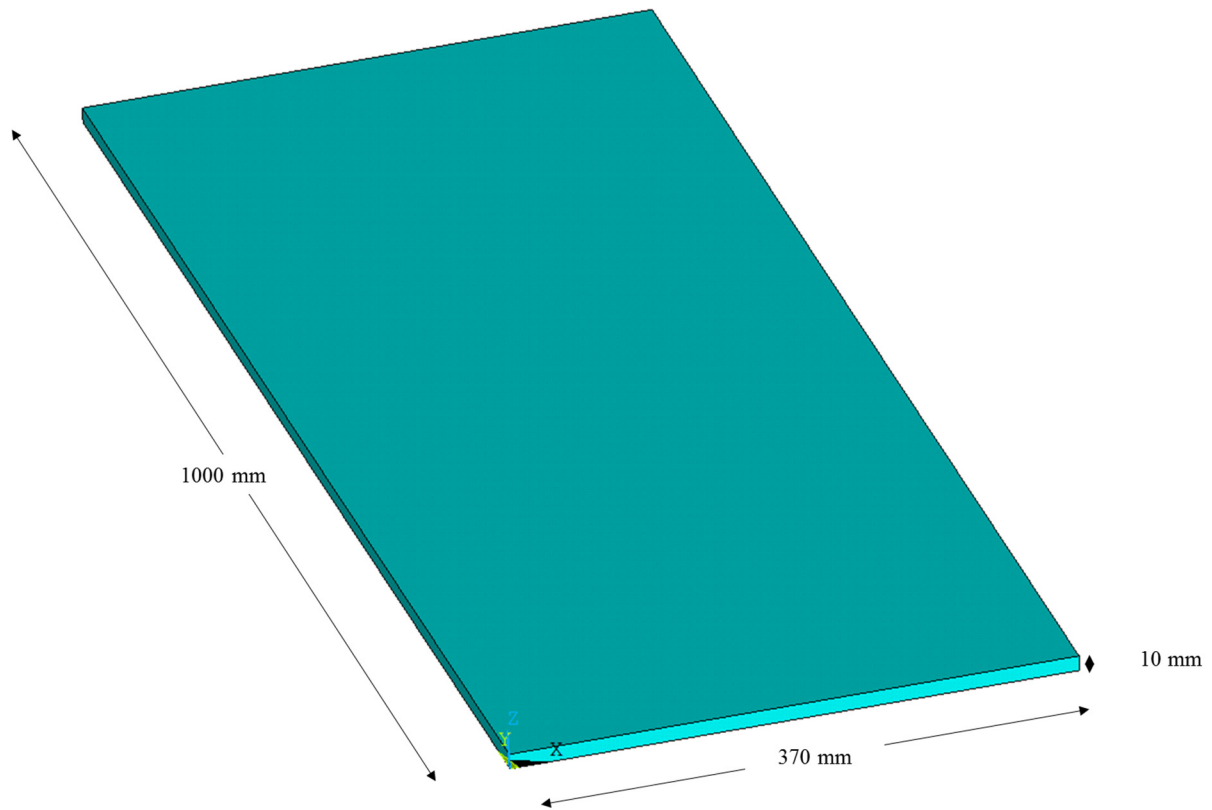

Figure 2: Component A

1000 mm
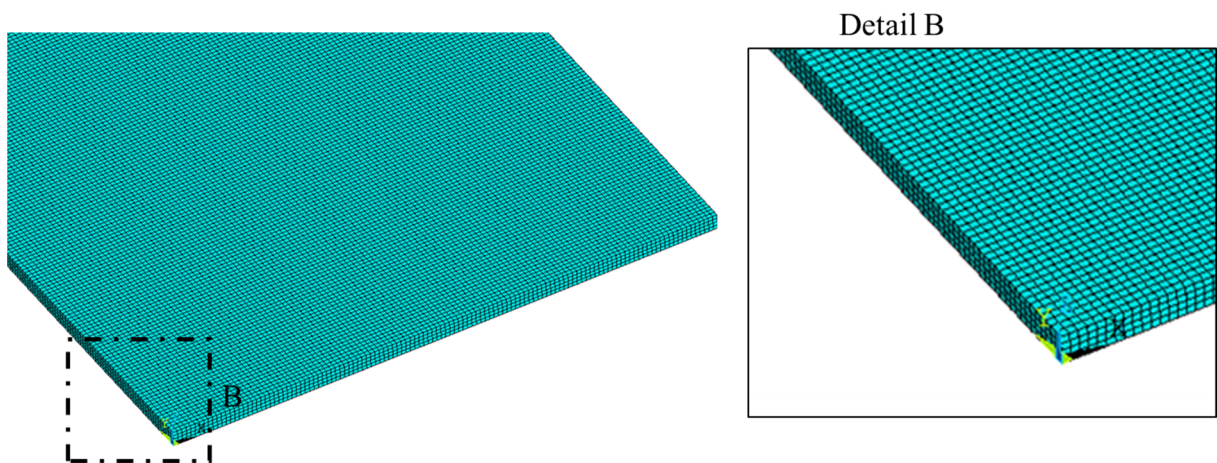
370 mm

10 mm
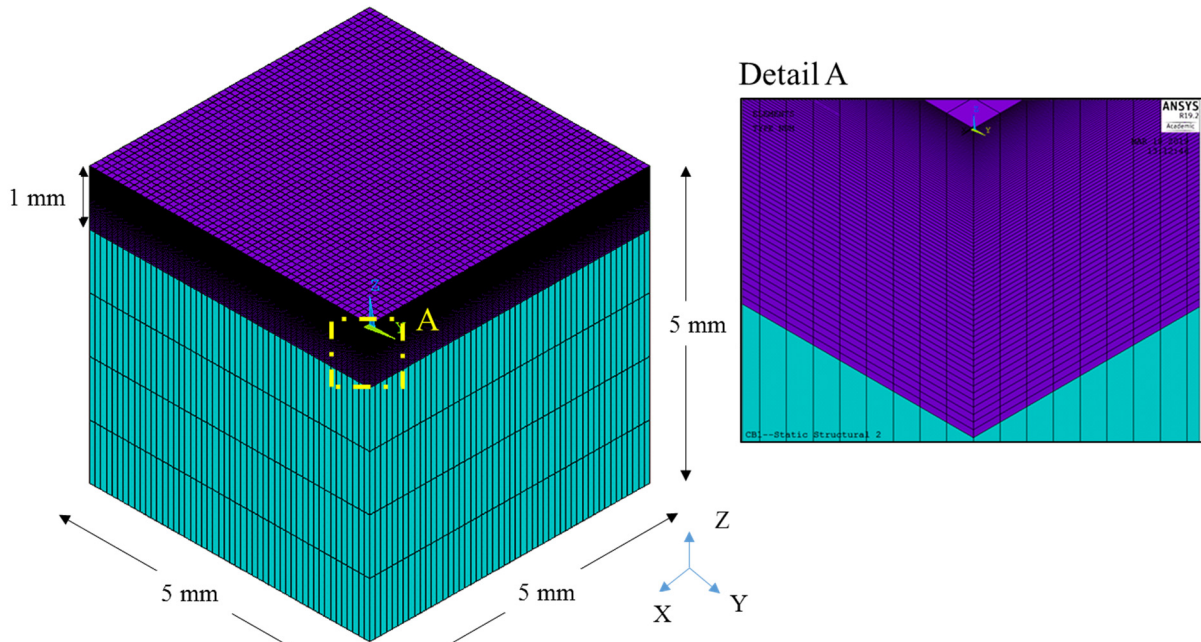
Figure 3: Component B

Detail B

Figure 4: Mesh of component B

3.3 Investigated materials

Effective material properties of 20MnCr5 and S355 were adopted from [8] and [1] respectively ν and α_{se} were assumed equal to 0.28 and 12 x 10^{-6} for both materials based on a range of values found in [11]. Bilinear elastic-plastic material models were applied for simulating the σ-ε behaviour taking into consideration the Bauschinger effect (kinematic hardening). The applied properties are presented in Table 1.

**Table 1**: Material properties of 20MnCr5 and S355

Material Property	20MnCr5	S355
E [MPa]	218,000	210,000
σ_y [MPa]	398	400
H [MPa]	2,261	2,330
v [-]	0.28	0.28
α_{se} [-]	12 x 10^{-6}	12 x 10^{-6}

3.4 Pseudothermal analysis

Commercial FE software ANSYS was applied for all simulations [12]. Temperature was applied as nodal loads for simulating the effect of shot blasting. For both components, solution was carried out in 3 steps. In the first one boundary conditions and loads were applied and in the second and third, the loads and the restraints were respectively removed.

In the case of component A, applied temperature on each node was a function of its depth. This was enabled through an appropriate function A(d) identical to the shape of the measured RS profile. The applied temperature on each node was equal to A(d), where d was the depth of the node, multiplied with the loading factor T_{load}. The values of 0.5, 1 and 2 are tested for this factor. Function A(d) is compared in Figure 5 with the RS profile measured in [6] for shot blasting. All the faces of the component apart from the top one were restrained to the direction normal to their plane, thus modelling a plate of infinite width.

In the case of component B and due to the unavoidably coarser mesh, such a distribution of temperature was not possible. Instead a universal differential temperature of -500 °C was applied at the nodes of the top and bottom face (both sides were shot blasted) for 50 mm in each direction adjacent to the centerline. Once again, all the faces of the component apart from the top one were restrained to the direction normal to their plane.
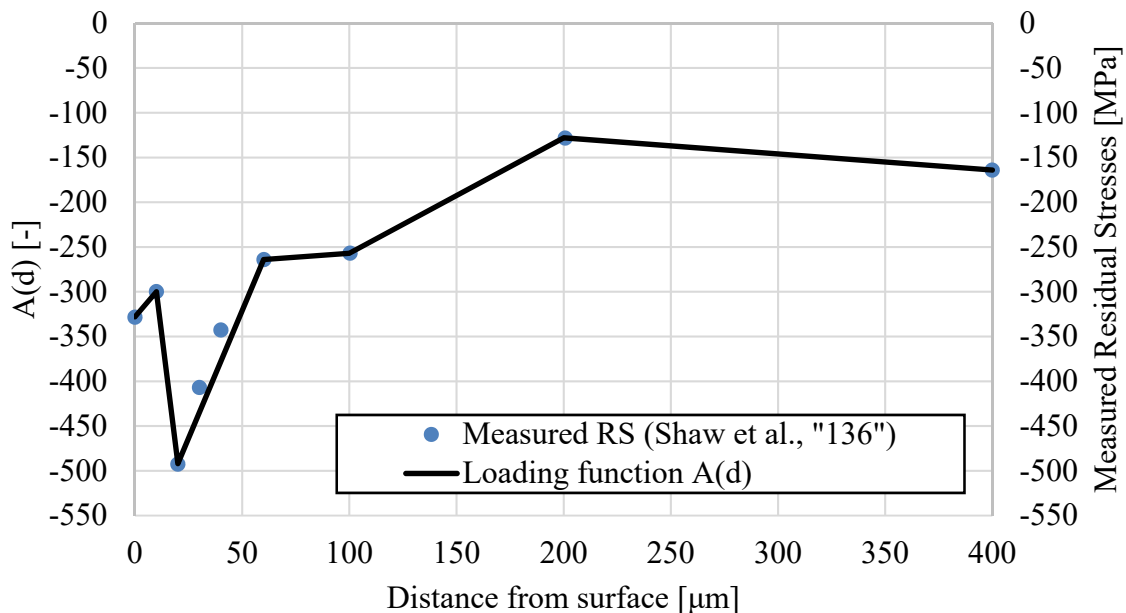
Figure 5: A(d) and RS measured in [3], both in depth direction

783

4 RESULTS AND DISCUSSION

4.1 Component A

The stress contours of component A for $T_{load} = 1$, prior and after removal of boundary conditions, are presented in Figure 6. The qualitative distribution of RS meets initial expectations with compressive stresses of large magnitude arising at the top face. Compressive stresses of lower magnitude are met in the rest component. As expected, removal of external restraints leads to stress relaxation on the boundaries of the component. However, the distribution of RS remains same qualitatively at its center. The through-depth profile of RS for the different values of T_{load} is presented in Figure 7 for better understanding.

In all three cases, the shift up of the RS profile due to stress relaxation after removal of restraints is evident. Nonetheless, it is expected that this effect is going to be negligible away from the boundaries for a larger component. Moreover, when a lager component is investigated, restraints of subsequent analyses could be applied for shot blasting as well and a removal of boundary conditions would not be necessary. A different effect of the restraints is expected in this case. For $T_{load} = 0.5$ the RS profile is qualitatively similar to the measured one but lies significantly higher. When the load is increased ($T_{load} = 1$ and 2) a plateau of RS near the surface is met, although temperature distribution followed the peaks and valleys of the measured RS according to function A(d). The introduced plasticity and the accompanied redistribution of stiffness is to be accounted for this inability of the numerical model to reproduce exactly the RS profile. The effect is becoming even more evident from the extension of the plateau when T_{load} is increased from 1 to 2, causing the widening of the plastic zone.

In any case, the method seems promising, as the calculated RS profile for $T_{load} = 2$ after removal of external restraints lies within the boundaries of the measured RS although the peaks and valleys are not reproduced. As it is mentioned above such a detailed analysis would be anyway impossible for a larger component due to mesh size restrictions.
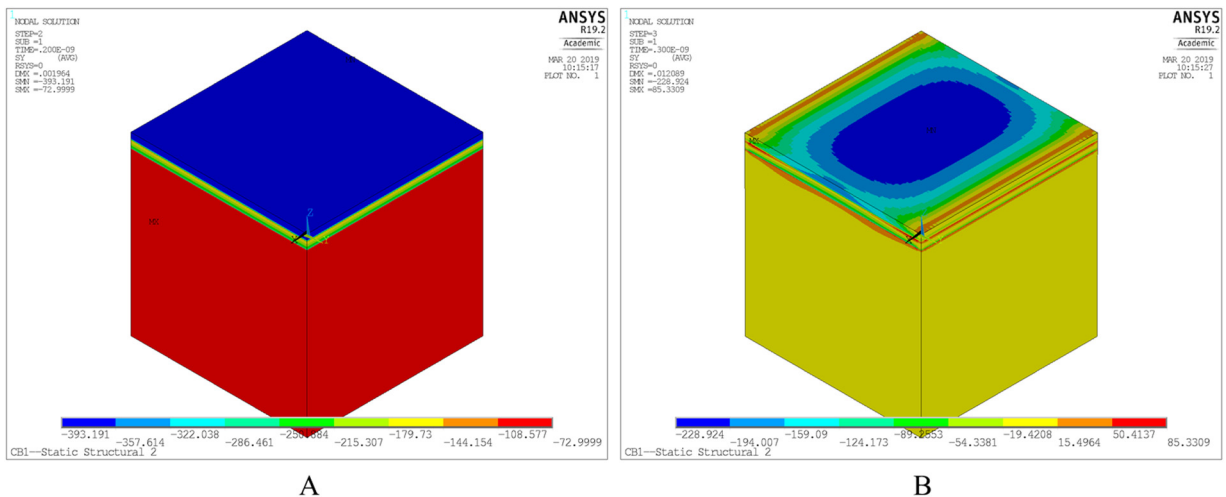

A   B

Figure 6: Component A – Contours of residual stresses introduced for $T_{load} = 1$, prior (A) and after (B) removal of restraints – results in N/mm^2
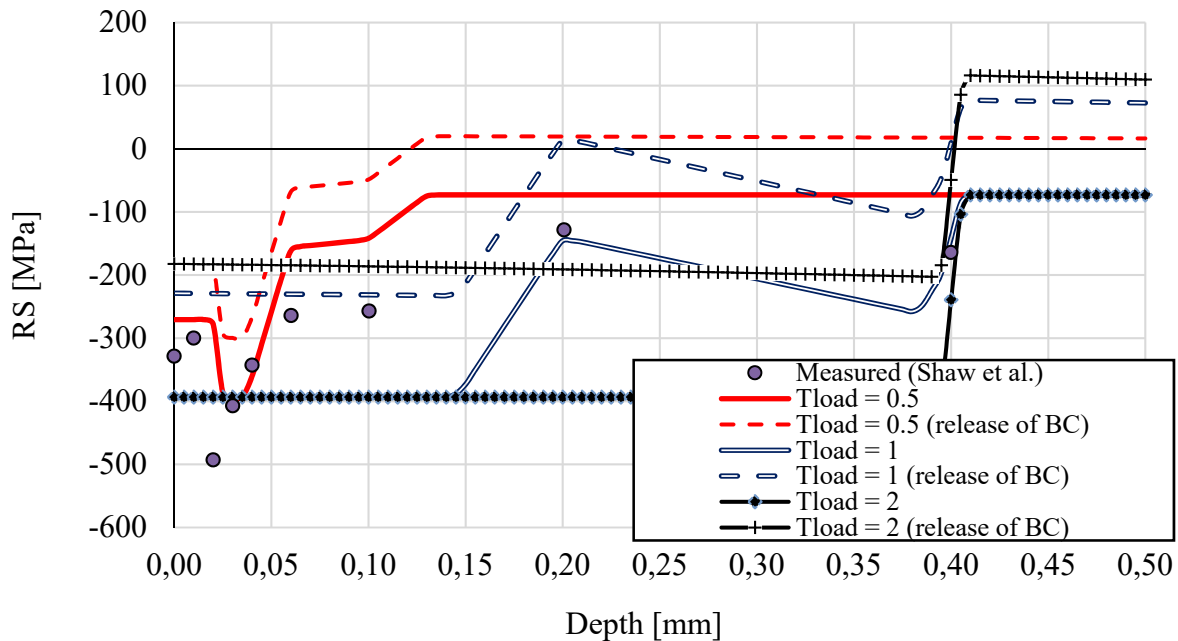
Figure 7: Component A – RS profile in depth direction at the center of the component

4.2 Component B

The countours of RS and Von Mises plastic strains for component B prior and after to the removal of external restraints are presented in Figure 8 and Figure 9 respectively. As expected compressive stresses are met on the surface of the area where differential temperature of –500 °C is applied. Comparing the two contours, the above-stated expectation that stress relaxation would not cause such a significant change at the center of a larger component is validated.

The through-thickness RS profile at the center of the specimen is illustrated in Figure 10, in order to enable a better overview. A linear, symmetric distribution of stresses is evident. It is as expected compressive near the outer surfaces and moves to the tensile region at a depth larger than 4 mm. Symmetry is attributed to the simultaneous application of the thermal loads on both upper and bottom faces. The residual stresses inner to the external upper and bottom faces, where the thermal load was applied, are introduced due to equilibrium reasons. As expected, the fluctuating profile of the measured RS cannot be reproduced due to the coarser mesh and homogenous surface loading. Nevertheless, compressive stresses of the same order of magnitude as those measured in [1] are introduced near the surface, without significant computational effort. Questions arise however, how an erroneous modelling of the RS at depths deeper than 1 mm, where measurements for validation are more difficult, could affect a subsequent simulation of WRS. Component's significant ratio of length to width is to be accounted for the higher magnitude of longitudinal stresses.
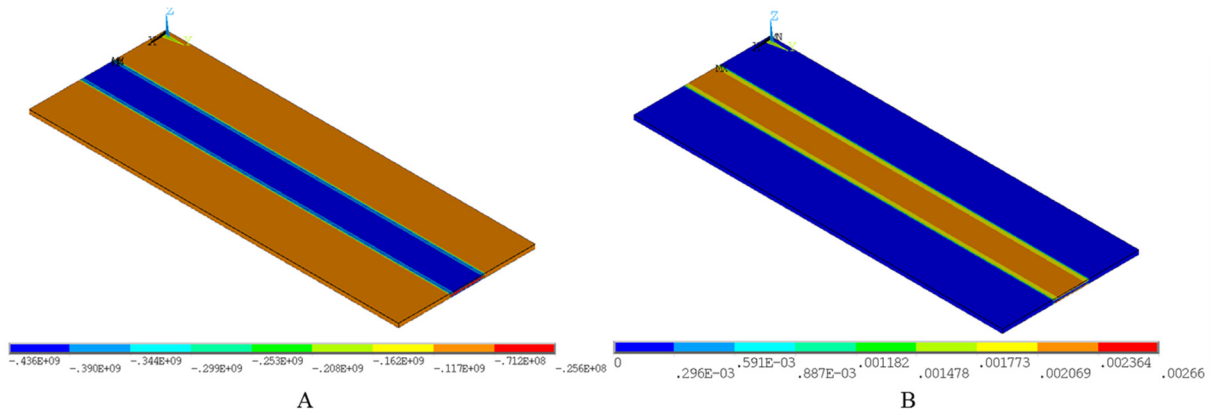
Figure 8: Component B, results prior to removal of restraints – A) Contours of residual stresses (results in N/m²) – B) Contours of Von Mises plastic strain
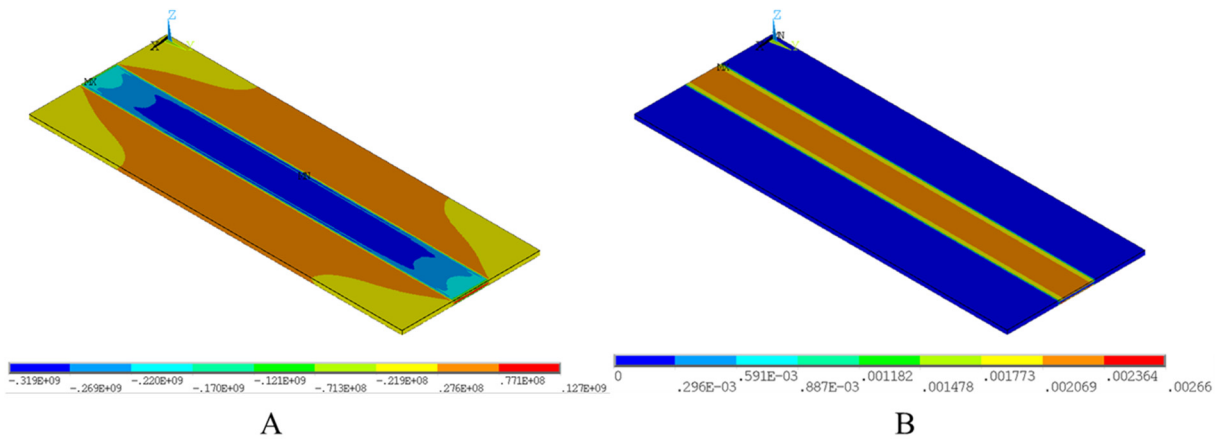

Figure 9: Component B, results after removal of restraints – A) Contours of residual stresses (results in N/m2) – B) Contours of Von Mises plastic strain
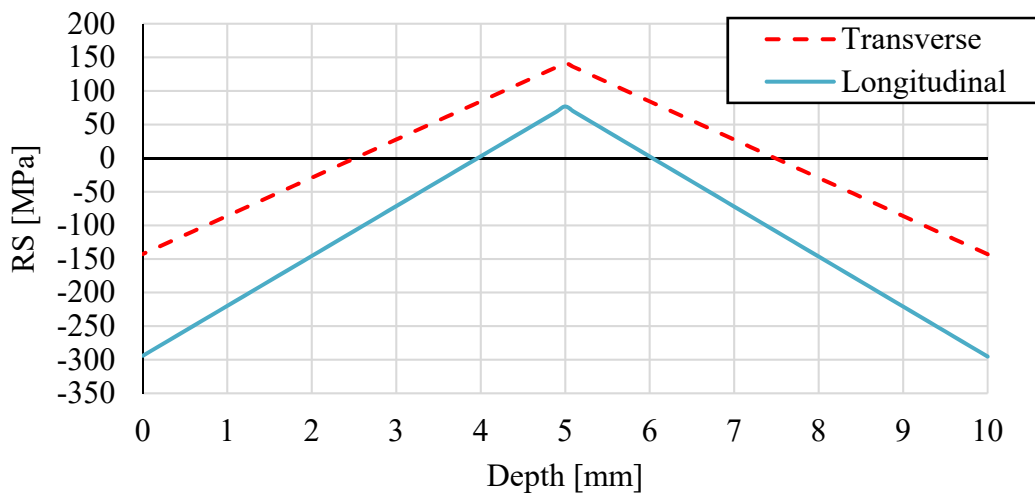

Figure 10: Component B – RS profile in depth direction at the center of the component

5 CONCLUSIONS AND FUTURE WORK

A pseudothermal modelling approach for introducing RS from shot blasting prior to welding simulations has been proposed and tested in the present study. Thermal strains are imposed on the upper layer of a component, so that the desired RS profile can be introduced. Significant simplifications have to be adopted, due to mesh restrictions, but the results seem promising. The influence of the RS from shot blasting is expected to be negligible in any case near the HAZ and FZ of weldments, as the welding heat input erases previously introduced plastic strains and RS. The current method could improve the agreement of simulated and measured RS profiles on shot blasted surfaces away from the weld section. Nevertheless, the following additional investigations are proposed for further validation and better calibration of the approach:

- Arbitrary restraints were applied in the present study, whose removal for subsequent simulations would influence significantly the RS profiles. This influence of stress relaxation was less significant for the larger component validating initial expectations. Additional analyses, with boundary conditions of subsequent welding simulations can be applied, in order to further test the influence of external restraints.

- Profile of measured RS could not be reproduced, even in the case where a very fine mesh was applied and therewith, pseudothermal loading with fluctuation in depth direction similar to the measurements could be applied. The nonlinear material behaviour lead to either underestimation of RS with qualitatively better agreement, or to introduction of RS quantitatively closer to the real ones but with different distribution. Nevertheless, this would not deter the application of the method on larger components as the above mentioned necessary mesh restrictions would anyway allow only the creation of a homogenous stress field at the top layer. Applying more complex or even fictitious material model could enable better agreement with measured profiles.

- Finally, a coupled simulation of shot blasting with a subsequent weld simulation is proposed, so that the improvement in the calculation of WRS can be documented is proposed.

6 ACKNOWLEDGEMENT

REFERENCES

[1] Schubnell J., Gkatzogiannis S., Farajian M., Knoedel P., Luke T., Ummenhofer T. *Rechnergestütztes Bewertungstool zum Nachweis der Lebensdauerverlängerung von mit dem Hochfrequenz-Hämmerverfahren (HFMI) behandelten Schweißverbindungen aus hochfesten Stählen.* (Computer-aided evaluation tool for the verification of fatigue life extension of the weldments of high strength steel post-weld treated with High Frequency Mechanical Impact (HFMI), final report in preparation) Abschlussbericht DVS 09069 – IGF 19227 N, Fraunhofer Institut für Werkstoffmechanik und KIT Stahl- und Leichtbau, Versuchsanstalt für Stahl, Holz und Steine, Freiburg und Karlsruhe 2019 (in Bearbeitung).

[2] Knoedel P., Gkatzogiannis, S., Ummenhofer T. Practical Aspects of Welding Residual Stress Simulation. *Journal of Constructional Steel Research* (2017) **132**: p 83-96.

[3] Gkatzogiannis S., Knoedel P., Ummenhofer T. Strain Rate Dependency of Simulated Welding Residual Stresses. *Journal of Material Performance and Engineering* (2017) **27**(10): pp. 5079-5085.

[4] Gkatzogiannis S., Knoedel P., Ummenhofer T. Influence of Welding Parameters on the Welding Residual Stresses. *Proceedings of the VII International Conference on Coupled Problems in Science and Engineering, Rhodes 12–14 June* (2017): pp. 767–778.

[5] Knoedel P., Gkatzogiannis S., Ummenhofer T. FE Simulation of Residual Welding Stresses: Aluminum and Steel Structural Components. *Key Engineering Materials* (2016) **710**: pp. 268-274.

[6] Shaw B. A., Korsunsky A. M., Evans J. T. Surface Treatment and Residual Stress Effects on the Fatigue Strength of Carburised Gears. *12th European Conference on Fracture (ECF-12), Sheffield, 14–18 September* (1998).

[7] Hensel J., Nitschke-Pagel T., Eslami H., Dilger K. *Fatigue Strength Enhancement of Butt Welds by Means of Shot Peening and Clean Blasting*. IIW Document XIII-2733-18 (2018).

[8] EN ISO 683-3:2019. *Heat-treatable steels, alloy steels and free-cutting steels -- Part 3: Case-hardening steels*

[9] Brnic J., Brcic M. Comparison of Mechanical Properties and Resistance to Creep of 20MnCr5 Steel and X10CrAlSi25 Steel. *Procedia Engineering* (2015) **100**: 84 – 89.

[10] Gkatzogiannis S. *Finite Element Simulation of Residual Stresses from Welding and High Frequency Hammer Peening* (working title). Doctoral Thesis, KIT, Karlsruhe Institute of Technology, Steel and Lightweight Structures, to be submitted in 2019.

[11] Avallone E. A., Baumeister T. M. *Marks' Standard Handbook for Mechanical Engineers*, 10th Edition (1996).

[12] ANSYS® Academic Research. Release 19.2, Help System, ANSYS, Inc. (2019).